ADVANCED OPTICAL MATERIALS
www.advopticalmat.de

Reduction of Non-Radiative Losses in Trap-Free Organic Light-Emitting Diodes by Dilution with A Large Bandgap Host

*Oskar Sachnik, Xin Zhou, Jawid Nikan, Bas van der Zee, Yungui Li, Paul W.M. Blom, and Gert-Jan A.H. Wetzelaer**

The emitter 9,9′,9′′-(5-(4,6-diphenyl-1,3,5-triazin-2-yl)benzene-1,2,3-triyl)tris (9*H*-carbazole) (3CzTRZ) seems an ideal candidate for efficient single-layer blue organic light-emitting diodes (OLEDs). It combines trap-free electron and hole transport with thermally activated delayed fluorescence (TADF) for triplet harvesting. However, in spite of the absence of charge trapping defects, neat films of 3CzTRZ suffer from a low photoluminescence quantum yield (PLQY) of only 40%. Time-resolved photoluminescence measurements reveal that the low PLQY results from the fact that next to fast intersystem crossing the rate for reverse intersystem crossing is very slow and nearly similar to the rate of non-radiative recombination of triplet excitons to the ground state. This loss process of non-radiative triplet decay is even more pronounced in OLEDs due to the 75% direct triplet-exciton formation, resulting in a low external quantum efficiency (EQE) of 4.5%. By diluting 3CzTRZ in a large bandgap host, the triplet lifetime is increased by at least an order of magnitude, resulting in an enhanced PLQY of 70% and a more than three-fold enhancement of the EQE to 15% in a single-layer blue OLED. Device simulations confirm that the increased EQE can be ascribed to an elongated triplet lifetime upon dilution of the emitter in a host matrix.

1. Introduction

Upon years of continuous research, organic light-emitting diodes (OLEDs) have emerged as one of the most advanced technologies for display applications.[1] In its most simple form, an OLED requires an organic semiconductor, sandwiched between an electron-injecting cathode and hole-injecting anode. However, a major problem for such a single-layer device is the presence of extrinsic defects in the organic semiconductor, such as oxygen and water.[2–5] Such defects have a triple negative effect on OLED efficiency: first, they trap charge carriers leading to non-radiative trap-assisted recombination.[6] Second, singlet excitons formed after bimolecular recombination of injected electrons and holes diffuse towards defects where they get quenched, resulting in a low photoluminescence quantum yield (PLQY).[7] Third, due to the unbalanced transport by trapping of electrons and/or holes the recombination zone is located close to one of the injecting electrodes, leading to a low outcoupling efficiency.[8] Consequently, the common perception is that a high efficiency can only be attained with the use of a multilayer OLED structure. In these multilayer structures, the recombination zone is confined in a thin emissive layer, surrounded by transport and blocking layers.[9,10] The incorporation of electron and hole-transporting layers compensates for injection issues from the contacts and for imbalanced charge transport that most organic semiconductors suffer from.[11] Additionally, exciton-blocking layers are introduced to prevent the migration and quenching of excitons.[12,13] Furthermore, the thin emissive layer can be placed in a position in the OLED that is optimal for light outcoupling.[14] As a result, most multilayer structures contain 5 or more layers, which prevents the use of solution processing due to stack integrity issues leading to enhanced fabrication costs. Furthermore, the more complex structure hinders optimization and understanding of degradation processes.

The prerequisite for an efficient OLED based on just a single layer of emitting material is the combination of ohmic contacts, trap-free balanced bipolar charge transport and efficient current-to-light conversion. Combination of all these properties sets a high demand on the selection of the organic semiconductor. Regarding trapping by extrinsic defects, we recently found that it is related to the energy levels of the organic semiconductor, the ionization energy (IE) and electron affinity (EA).[15] For IEs higher than 6.0 eV, hole trapping by water clusters limits the hole

O. Sachnik, X. Zhou, J. Nikan, B. van der Zee, Y. Li, P. W. Blom, G.-J. A. Wetzelaer
Max Planck Institute for Polymer Research
Ackermannweg 10, 55128 Mainz, Germany
E-mail: wetzelaer@mpip-mainz.mpg.de

The ORCID identification number(s) for the author(s) of this article can be found under https://doi.org/10.1002/adom.202302000

DOI: 10.1002/adom.202302000

transport, whereas for EAs lower than 3.5 eV, electron transport is hindered by trapping due to oxygen-related defects.[4,16] Therefore, the energy levels of an organic semiconductor have to be situated within this energy window to enable trap-free electron and hole transport. The organic semiconductor (9,10-bis(4-(9*H*carbazol-9-yl)−2,6-dimethylphenyl)−9,10-diboraanthracene (CzDBA) with a bandgap of 2.5 eV has its energy levels located exactly at the edges of this trap-free energy window, resulting in nearly trap-free and balanced electron and hole transport.[17,18] Combined with a high PLQY (≈90%) and triplet harvesting by thermally activated delayed fluorescence (TADF), an efficient OLED with 19% external quantum efficiency was realized with a simplified structure.[18,19] Here, next to the single emissive CzDBA layer, two tunnel barriers were applied to ensure Ohmic contacts, which next to efficient charge injection also prevent quenching of charges at the electrodes due to band bending.[20] However, the width of ≈2.5 eV of the trap-free energy window poses a fundamental limit for realizing trap-free transport in organic semiconductors with a bandgap larger than 2.5 eV, as required for blue-emitting OLEDs, where typically a bandgap of ≈3 eV is needed.

Recently, we presented a strategy to overcome this challenge, by spatially separating the electron and hole transporting part of an organic semiconductor having its EA outside of the trap-free window. The molecular design then enables the organic semiconductor to stack in such way, that the electron transporting part, where the lowest unoccupied molecular orbital (LUMO) is located, is protected from trap-related sources by the surrounding hole transporting part, where the highest occupied molecular orbital (HOMO) is located.[21] The most promising candidate found in that study is 9,9′,9′′-(5-(4,6-diphenyl-1,3,5-triazin-2-yl)benzene-1,2,3-triyl)tris(9*H*-carbazole) (3CzTRZ), a compound with a bandgap close to 3.0 eV and a practically trap-free electron and hole transport.[21,22] As previously demonstrated, the absence of electron and hole trapping realizes perfectly balanced charge transport in 3CzTRZ (**Figure 1**).[21]

Furthermore, due to its spatial separation of HOMO and LUMO orbitals, 3CzTRZ not only exhibits remarkable electrical properties, but also displays TADF by reverse intersystem crossing (rISC). Combination of these beneficial characteristics and the simultaneous large bandgap make it a promising candidate for an efficient blue single-layer OLED.

We note that 3CzTRZ previously has been used successfully in a multilayer structure.[22–24] In a multilayer device architecture, however, the charge transport is of lesser importance, as the charges are confined to the emissive layer by means of blocking layers.[25] The drawback of this architecture is that it is more complicated to design, fabricate and understand, while the use of additional heterojunctions also negatively impacts the operating voltage.[26,27] Furthermore, in the emissive layer 3CzTRZ has been used as a guest emitter inside a host, although it is unclear what the role of this host material is in the final OLED performance.[22] Hosts are typically used in OLEDs to impact charge transport and reduce "concentration quenching", although there is frequently no clear understanding which physical mechanism underlies the improvement in OLED performance.[28,29]

Here, we investigate the use of 3CzTRZ in single-layer OLEDs, based on the excellent balanced charge transport characteristics

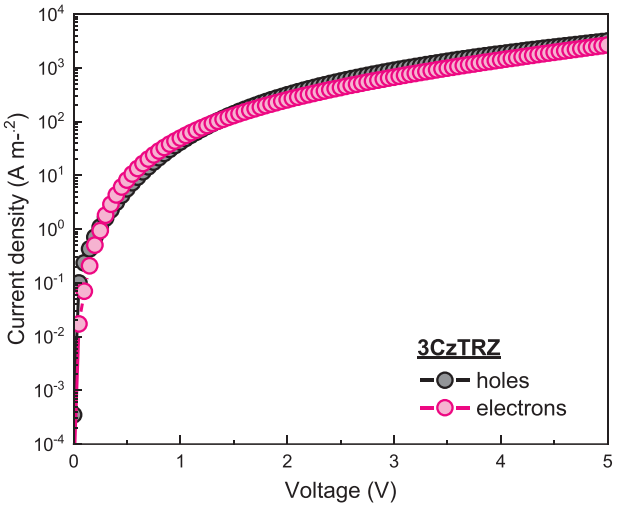

Figure 1. Current density (*J*)- voltage (*V*) characteristics of a hole-only and electron-only device of a neat layer 3CzTRZ with 98 nm thickness.[21] The employed device structures of the electron- and hole-only devices utilize either an ohmic electron (3CzTRZ / TPBi (4 nm)/Ba (5 nm)/Al) top contact or an ohmic hole (3CzTRZ /C_{60}/MoO_3/Al) top contact, respectively. The obtained perfectly balanced charge transport of 3CzTRZ makes it a potential candidate for a single-layer organic light-emitting diode.

of this TADF emitter. We demonstrate that the PLQY in the neat film is low, mainly arising from a short triplet-exciton lifetime, which reduces the contribution of delayed fluorescence via reverse intersystem crossing. Under electrical excitation, this effect reduces the efficiency even further, as 75% of the generated excitons are initially triplets. Interestingly, the triplet lifetime is vastly increased when 3CzTRZ is incorporated in a host, leading to enhanced triplet utilization and a more than threefold enhancement of the EQE.

2. Results and Discussion

To further investigate the suitability of 3CzTRZ for single-layer blue OLEDs, we performed photoluminescence quantum yield (PLQY) measurements of the neat film.[30] Surprisingly, in spite of the near absence of charge trapping defects at which excitons might dissociate, 3CzTRZ exhibits a relatively low PLQY of only 40% in a neat film (**Table 1**). For single-layer OLEDs with balanced charge transport, meaning that the recombination zone peaks in the middle of the layer, an outcoupling efficiency to air in the range of 25–26% is expected.[8] Together with a PLQY of ≈40% an external quantum efficiency (EQE) of ≈10–11% is therefore expected for the 3CzTRZ OLED.

As a next step, we have fabricated an OLED based on a single layer of 3CzTRZ sandwiched between an ohmic hole and electron contact (**Figure 2a**). As a bottom hole-injecting contact we chose PEDOT:PSS:PFI, which was recently demonstrated to provide ohmic hole injection into organic semiconductors with IEs up to ≈5.9 eV.[31] To ensure ohmic electron injection, we used a top contact configuration comprising a thin (4 nm) TPBi interlayer as a tunnel barrier between the emissive organic semiconductor and metal cathode 1.[32]

Table 1. Summarized PL decay results obtained by numerical fitting.

	k_{ISC} [s^{-1}]	k_{rISC} [s^{-1}]	τ_t [s]	τ_s [s]	k_{TTA} [m^3 s^{-1}]	$PLQY_{exp}$ [%]	$PLQY_{sim}$ [%]
100%	4×10^7	8.5×10^4	1.5×10^{-5}	8×10^{-8}	6×10^{-19}	40%	35%
50%	4×10^7	1.5×10^5	$\geq 1.0 \times 10^{-4}$	1.5×10^{-7}	6×10^{-20}	69%	60%

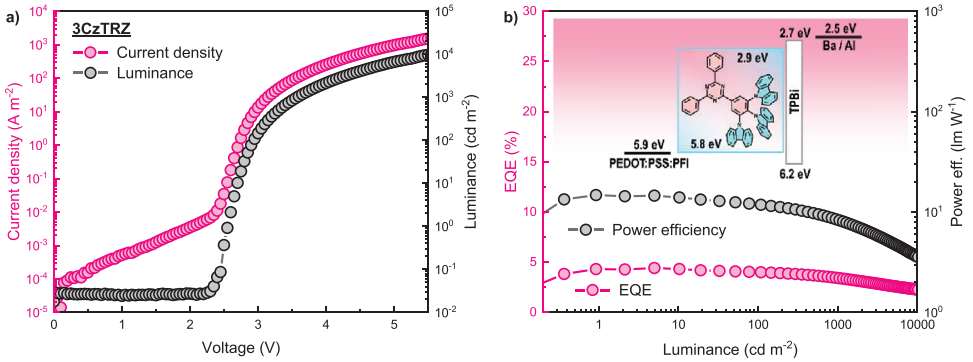

Figure 2. a) Current-density-voltage *(J–V)* and luminance-voltage *(L–V)* characteristics of a single-layer OLED of 3CzTRZ with 82 nm thickness b) corresponding EQE and power efficiency. The inset shows a schematic device layout of the single-layer OLED. The emissive layer is sandwiched between a PEDOT:PSS:PFI bottom anode and a barium/aluminum top cathode. To facilitate electron injection, a thin TPBi (4 nm) interlayer between emissive layer and top contact is inserted. The work functions of the electrodes and other energy levels are indicated.

The resulting device performance based on a simple layer of 3CzTRZ is displayed in Figure 2a,b. A turn-on voltage of 2.54 V at 1 cd m^{-2} is observed, which is lower than the optical bandgap (2.95 V) and is due to the recombination of diffused charge carriers below the built-in voltage.[33] The device reaches a luminance of 100 cd m^{-2} at 3.10 V and 1000 cd m^{-2} at 4.65 V. The maximum EQE of 4.5% is considerably lower than expected from considerations based on the PLQY and outcoupling efficiency, resulting in a low power efficiency of 24 lm W^{-1}. Summarizing, in spite of the absence of charge trapping defects both PLQY and EQE of the 3CzTRZ single-layer OLEDs are far below expectations.

To elucidate the origin of the low PLQY and EQE we performed time-resolved photoluminescence (TRPL) measurements on 3CzTRZ thin films. The PL decay curve is shown in Figure 3a (red symbols). The measurements are simulated using rate equations for the singlet and triplet exciton density, given by

$$\frac{d[S]}{dt} = [S_0] - \frac{[S]}{\tau_s} - k_{ISC}[S] + k_{rISC}[T] + 0.25k_{TTA}[T][T] \quad (1)$$

$$\frac{d[T]}{dt} = -\frac{[T]}{\tau_T} + k_{ISC}[S] - k_{rISC}[T] - 1.25k_{TTA}[T][T] \quad (2)$$

with $[S_0]$ the initial singlet density, τ_s and τ_t the singlet and triplet lifetime, k_{TTA} the triplet-triplet annihilation rate constant, k_{rISC} the reverse intersystem crossing rate, and $[S]$ and $[T]$ the singlet and triplet concentration, respectively.[34] Typically, the prompt fluorescence (τ_{PF}) is attributed to the singlet lifetime τ_s and rep-

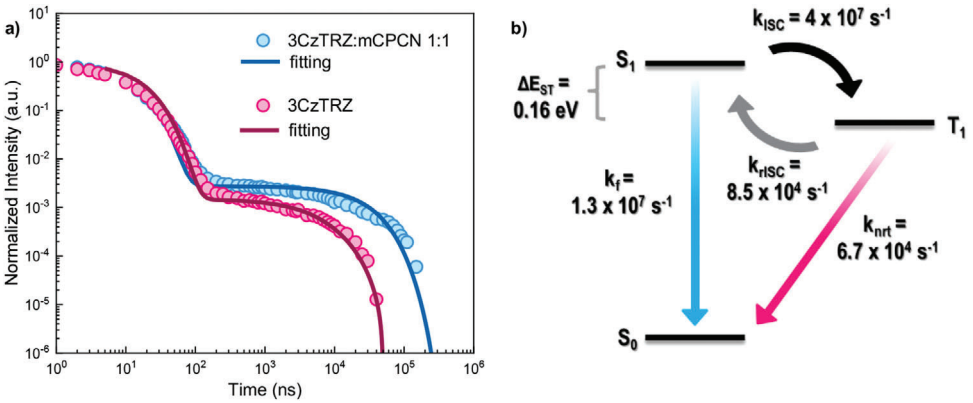

Figure 3. a) Transient photoluminescence decay measurement of neat 3CzTRZ (red) and 3CzTRZ:mCPCN (1:1) blend (blue) in film. Dots represent the experimental data and lines represent the fit obtained by a numerical model.[34] b) Characteristic time constants of the photophysical processes of the neat 3CzTrz film.

resents the decay to the ground state S_0 of excitons that initially populate S_1. The delayed fluorescence (τ_{DF}) arises from fluorescence that occurs as a result of the repopulation of S_1 by T_1 via rISC. The simulation is shown in Figure 3a as a solid line and the fit parameters are given in Table 1. With the addition of a small contribution of triplet-triplet annihilation we reproduce both the decay as well as the PLQY, determined by the area under the curve.

To put the photophysical processes in perspective, we plot in Figure 3b the characteristic time constants of each process in a schematic energy diagram. From fitting the PL decay, it is observed that the prompt fluorescence lifetime (τ_{PF}) of 18 ns is mainly governed by the fast ISC process, with the lifetime limited by intersystem crossing to the triplet state, rather than decay of the singlet state, for which the lifetime is determined to be 80 ns. Shortening the singlet lifetime in the modelling at the expense of the intersystem crossing rate would lead to an insufficiently intense delayed fluorescence signal, implying that the intersystem crossing rate must be fast. On the other hand, the reverse intersystem crossing process is very slow and nearly equal to the inverse of the triplet lifetime, implying a high chance of nonradiative decay of the triplet state. The delayed fluorescence lifetime (τ_{DF}) is entirely limited by the triplet lifetime τ_T, which can therefore be reliably obtained from fitting the PL decay. The relatively high intersystem crossing rate combined with the low reverse intersystem crossing rate, implies in practice that in the event of one triplet *to* singlet up-conversion, almost 10^3 singlet excitons experience down-conversion to the non-emissive triplet-state. For 3CzTRZ a singlet-triplet gap (ΔE_{ST}) of 0.16 eV was reported, which is relatively large and is most likely the origin of the low k_{rISC} rate.[22] The fact that $1/k_{ISC}<\tau_s$ has the consequence that even after a triplet has been upconverted from T_1 to S_1 it has a bigger chance to fall back to T_1 instead of radiatively recombining to S_0. Combined with the slow rISC rate, the triplet state T_1 stays therefore heavily populated over a long time period. This, combined with the fact that the non-radiative triplet decay τ_T is almost equally fast as the rISC process then explains the low PLQY of 3CzTRZ.

The large population of the triplet state and resulting non-radiative losses via recombination of triplets to the ground state also has consequences for the analysis of the OLED efficiency. Typically, to rationalize the OLED efficiency, the product of the electrical efficiency, spin statistics (100% for TADF), outcoupling efficiency and PLQY is calculated. However, in the case that non-radiative losses of triplet excitons play an important role, as is the case for 3CzTRZ, this analysis is not correct. In a PLQY experiment, 100% singlets are generated as a starting point, of which a certain fraction is then transformed into triplets via ISC. In contrast, in an OLED, 75% of the excitons are directly generated as triplets, meaning that the overall triplet density and therefore non-radiative losses of triplets is different for both experiment, as also recently noted by Ruhstaller et al.[35] In other words, the PLQY is not necessarily equal to the electroluminescence quantum yield (ELQY). In **Figure 4** we have plotted the calculated PLQY and ELQY for 3CzTRZ as a function of the rate of non-radiative triplet recombination k_{nrt}. The PLQY and ELQY are here determined by starting with initially 100% singlet excitons and a 1:3 singlet-to-triplet ratio, respectively, using the method of Ruhstaller et al.[35] For low rates (long triplet lifetimes), the triplets

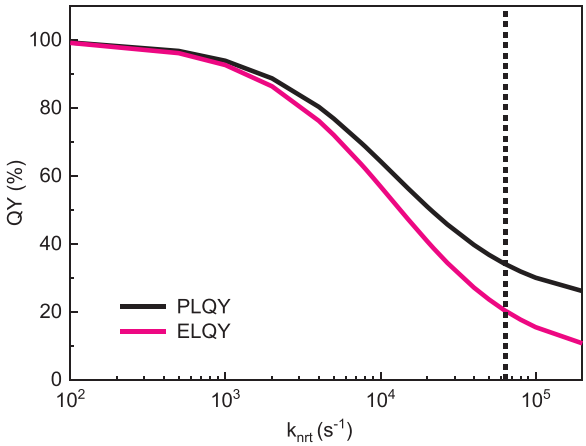

Figure 4. ELQY and PLQY for the 3CzTRZ emitter plotted versus k_{nrt}. The solid vertical dotted line corresponds to the value of k_{nrt} from fitting the TRPL.

are mainly depleted via rISC, and non-radiative recombination of triplets does not play a role, such that PLQY equals ELQY. With increasing rate, a difference between PLQY and ELQY starts to evolve. When assuming $k_{nrt} = 1/\tau_T$, the experimentally obtained triplet lifetime yields a k_{nrt} of 6.7×10^4 s^{-1}, corresponding to an ELQY of only 20%, and a PLQY of 34%. Additionally, the PLQY may also be influenced by additional nonradiative singlet decay, which was omitted in the calculations in Figure 4 for simplicity. Most importantly, the analysis in Figure 4 reveals that when the PLQY of a TADF emitter is limited by the non-radiative decay of triplet excitons, it cannot be used as a simple factor to calculate the external quantum efficiency: based on the PLQY, an EQE of ≈10% would be expected for the 3CzTRZ OLED, when considering an optical-outcoupling efficiency of 25%, whereas the measured value is only 4.5%, which matches the EQE as expected from the low ELQY of 20%

A further enhancement of the ELQY and PLQY of 3CzTRZ would thus require an elongation of the triplet lifetime τ_T. A common strategy to prevent loss processes, such as concentration quenching or interactions between triplet and/or singlet excitons is the adjustment of the molecular structure in such way, that an increase in the intermolecular distance is achieved, e.g., by incorporation of bulkier side groups.[36] Although such strategies typically offer improvements in reduction of the concentration quenching and increase of the PLQY, a major downside is that a simple change in the molecular structure can have tremendous influence on the intrinsic charge transport. In our study, the incorporation of *tert*-butyl groups on the carbazole donor-part resulted in a large imbalance of the charge transport, with the hole-transport being almost 2 orders of magnitude higher than the electron-transport (Figure S1, Supporting Information). Even though this adjustment offered improvements in the PLQY (up to 79%), the imbalanced charge transport will lead inevitably to an even worse OLED performance as most of the recombination then happens close to the cathode, resulting in a low outcoupling efficiency.

Another successful strategy to increase the intermolecular separation is the incorporation of a host-matrix which enables the dilution of the emitter.[37–39] The host typically has a larger

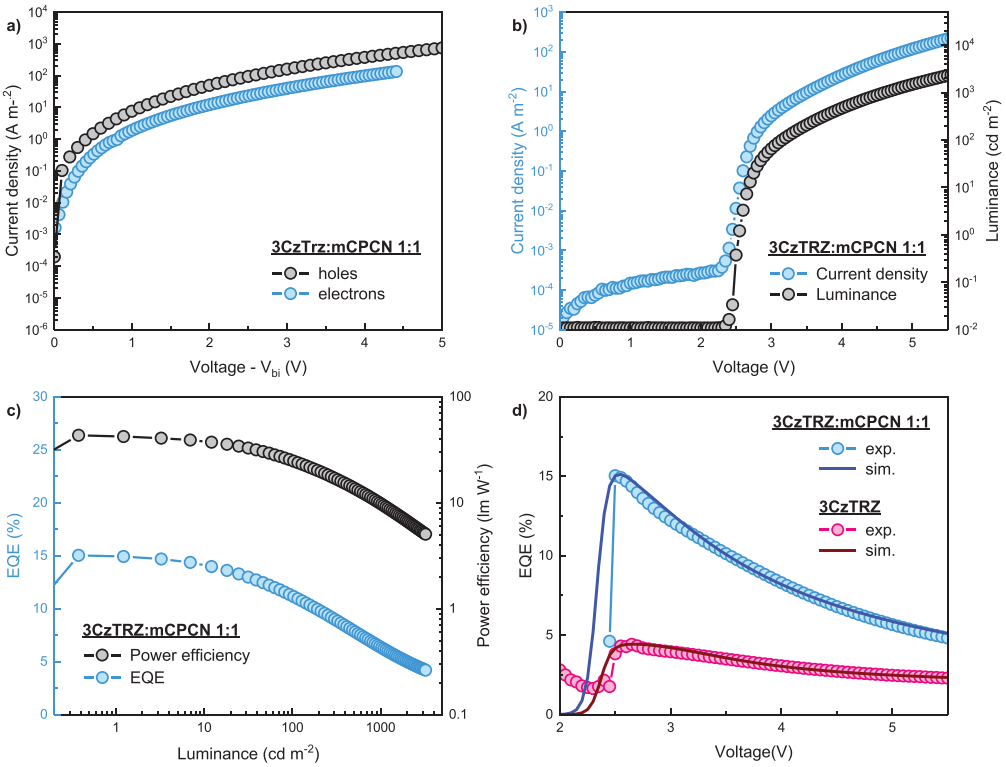

Figure 5. a) *J–V* characteristics of hole- and electron-only of 3CzTRZ:mCPCN (1:1) with 72 nm thickness. The voltage of the electron-only device was corrected for a built-in voltage V_{bi} of 0.63 eV.[40] b) *J-V-L* characteristics of a single layer 3CzTRZ:mCPCN (1:1) OLED with a PEDOT:PSS:PFI/3CzTRZ:mCPCN (72 nm)/TPBi (4 nm)/Ba (3 nm)/Al device layout. c) Corresponding EQE and power efficiency. d) EQE versus voltage of both OLEDs of pristine 3CzTRZ and 3CzTRZ:mCPCN (1:1). The experimental data is plotted as symbols, whereas the lines represent simulations with a drift-diffusion solver. The simulated singlet-generation efficiency is multiplied by a factor of 0.16 to obtain the EQE.

bandgap than the guest, and for sufficiently high concentration of the guest the transport of holes and electrons is carried exclusively by the guest. In this way, the balanced charge transport of 3CzTRZ, although diluted, can be preserved. We chose mCPCN (9-(3-(9*H*-carbazol-9-yl)phenyl)−9*H*-carbazole-3-carbonitrile) as a host-matrix because of its large bandgap of 3.6 eV and its previous successful employment in a single-layer OLED structure.[31] For 3CzTRZ, a simple 1:1 dilution showed already an improvement of the film PLQY, reaching 70% under nitrogen atmosphere, which is a strong indication for the reduction of non-radiative loss-processes. A similar PLQY enhancement was previously observed by Lee et al. by doping 3CzTRZ in DPEPO (bis[2-(diphenylphosphino)phenyl]ether oxide), which yielded a quantum yield of close to 100% in a 3:7 (3CzTRZ:DPEPO) dilution.[22] We also analyzed the TRPL of the 1:1 diluted film to quantitatively understand the increase of the PLQY. Measurements and the simulations are shown in Figure 3a (blue symbols), the resulting fit parameters are given in Table 1.

We observe an identical decay of both films up to 100 ns, which indicates that the prompt fluorescence is not affected by the dilution. In turn, this means that the singlet lifetime τ_S and intersystem crossing rate k_{ISC} that govern τ_{PF} are identical for the pristine and diluted film. Furthermore, the cross-over point from prompt- to delayed fluorescence is also hardly affected, meaning that k_{rISC} is also not strongly affected by dilution. At longer times, however, we see a strong increase of the delayed fluorescence in the doped film. As mentioned above, the delayed fluorescence is heavily influenced by the availability of excited triplet states, which can undergo up-conversion to emissive singlets. From the modelling of the TRPL we obtain an at least one order of magnitude higher triplet lifetime in the doped film, which is a direct result of the dilution of excited triplets. It is observed that the delayed fluorescence lifetime is no longer limited by the triplet-exciton lifetime. The longer triplet lifetime then allows more triplets to be upconverted to the S_1 state, resulting in a higher PLQY. Also, for the diluted film, the simulated PLQY agrees well with the experimentally obtained value. For the obtained τ_T of 10^{-4} s, according to Figure 4, an ELQY of ≈57% would be expected, meaning that as compared to the pristine 3CzTRZ OLED a threefold increase of the EQE is expected.

While maintaining trap-free charge transport and now with improved photophysical properties, we fabricated a single-layer OLED of 3CzTRZ doped in the mCPCN matrix. The resulting *J-V-L* characteristics in **Figure** 5b reveal a similar turn-on voltage of 2.54 V compared to the neat film device, as would be expected for direct charge injection into the emitter. The doped device reaches a luminance of 100 cd m^{-2} at 3.2 V and 1000 cd m^{-2} at 4.6 V. Interestingly, similar voltages need to be applied to achieve the same brightness as in the neat film device. Normally, upon dilution an increase in the operating voltage would be expected. A closer look reveals that indeed only half of the current is passed

through the diluted sample at the same voltage, which is a direct result of a lower charge mobility due to separation of charge transport sites. Nevertheless, we observe that the same amount of light is being generated at a given voltage, which results from an enhanced ELQY. Even though less charges are present in the diluted sample, the excited triplet states have more time to undergo the RISC process and decay by light emission as already demonstrated by our TRPL results. The benefits of dilution are also represented in the corresponding EQE and power efficiency (Figure 5c), which experience the expected threefold enhancement to 15% and 43 lm W^{-1}, respectively (Figure 5d). These results confirm that embedding a balanced emitter in a host-matrix of larger bandgap constitutes an effective option to enhance the TADF efficiency and ultimately the device performance.

To analyze the EQE versus voltage characteristics in more detail, we have simulated the OLEDs with a recently developed drift-diffusion model for TADF OLEDs.[41] First, the *J–V* characteristics are simulated based on the electron and hole mobility obtained from the charge-transport measurements. The drift-diffusion simulations then solve the recombination rate, and therefore exciton density, as a function of position in the device. Subsequently, the singlet-generation efficiency as a function of voltage is obtained by implementing the experimental photophysical parameters, including the exciton lifetimes, the rISC rates, and triplet-triplet annihilation. Multiplying the singlet-generation efficiency with a factor that includes the optical outcoupling and the radiative decay of singlet excitons then gives the EQE. For the neat 3CzTrz-based OLED, the maximum singlet-generation efficiency amounts to only 27% (Figure S3d, Supporting Information), being the result of the nonradiative decay of triplet excitons due to the short triplet lifetime, as determined from the PL experiment. This low internal efficiency therefore explains the low EQE of only 4.5%. In addition, the efficiency roll-off can be entirely reproduced without any fit parameters and is governed by the experimental triplet-triplet annihilation rate.

For the 3CzTrz:mCPCN OLED, the maximum singlet-generation efficiency is drastically increased up to 70% to 93% (Figure S4d, Supporting Information), which is entirely due to the increased triplet lifetime, resulting in an increased amount of triplet excitons converted to the singlet state via rISC. Only a range in singlet-generation efficiency can be given, since only a minimum value for the triplet lifetime can be estimated from the PL decay. Nevertheless, the greatly enhanced singlet-generation efficiency due to the increased triplet lifetime is in accordance with the threefold enhancement in EQE of the OLED upon dilution in a host matrix. The efficiency-roll of is also reproduced, but requires additional triplet-polaron quenching to match the shape of the EQE-*V* curve. This observation is tentatively explained by the reduction of triplet-triplet annihilation in the diluted film, in turn increasing the relative importance of other annihilation effects, such as triplet-polaron quenching.

We note that further dilution of the emitter (1:2) leads to a further improvement of the PLQY (99%), but at the same time to a larger imbalance in the electron and hole transport (Figure S2a, Supporting Information). The resulting reduction of the outcoupling efficiency nearly compensates the increase in PLQY, such that only a limited further improvement in the device performance is achieved (Figure S2c, Supporting Information, 17% EQE and 46 lm W^{-1}).

3. Conclusion

In conclusion, we have demonstrated that the electrical quantum efficiency of OLEDs based on the emitter 3CzTRZ is improved by reduction of the nonradiative triplet decay rate upon dilution of the emitter in a large gap host. The combination of trap-free transport and TADF makes 3CzTRZ a promising candidate for single-layer OLEDs. However, even though having promising electrical properties, pure 3CzTRZ suffers from a low PLQY of 40% in the solid film and, unexpectedly, a comparatively even lower EQE of only 4.5% in a single-layer OLED. We performed TRPL measurements, which revealed that 3CzTRZ mainly suffers from an imbalance of k_{ISC} and k_{RISC}, with k_{ISC} being almost 3 orders higher due to the large ΔE_{ST} of 0.16 eV. Since k_{RISC} is close to the rate of non-radiative recombination of triplets to the ground state, the majority of generated singlet excitons are converted to the triplet state and decay from there non-radiatively. In an OLED, this effect is even further amplified since 75% of the excitons are directly generated in the triplet state.

By doping 3CzTRZ in a large bandgap matrix, the triplet lifetime is extended by at least one order of magnitude and the PLQY is improved to 70%. Incorporated in a single layer OLED, the 3CzTRZ:mCPCN guest-host system showed a threefold enhancement of the EQE to 15%. The doped film of 3CzTRZ exhibits similar operating voltages to the neat film, even though less current is passed through the layer, giving rise to a high power efficiency of 43 lm W^{-1}. Through a combination of transient PL measurements and drift-diffusion device simulations, we show that the enhanced OLED performance upon dilution of 3CzTRZ in a mCPCN matrix is due to an elongated triplet-exciton lifetime.

These results demonstrate the effect of using a host-guest system beyond what is commonly referred to as "concentration quenching". In this case, the host elongates the triplet-exciton lifetime, which enhances the utilization of triplet excitons via reverse intersystem crossing, resulting in increased delayed fluorescence. This is effect is amplified in a working OLED, as under electrical excitation 75% of the formed excitons have a triplet character. Future work should focus on how the chemical structure of hosts impacts triplet utilization, which could improve finding and designing suitable host-guest combinations beyond a trial-and-error approach.

4. Experimental Section

Materials: 3CzTRZ was synthesized according to literature and purified by sublimation.[21] Nafion (PFI) was purchased from Sigma Aldrich as 5 wt.% solution in a mixture of lower aliphatic alcohols and water, containing 45% water. mCPCN, TPBi, and C_{60} were purchased in sublimed grade from Ossila BV. The thin film samples were prepared by evaporation to result in thicknesses of ≈100 nm.

Device Fabrication: OLED devices were fabricated on glass substrates prepatterned with ITO. The substrates were cleaned by washing with detergent solution and ultrasonication in acetone (5 min) and isopropyl alcohol (5 min), followed by UV–ozone treatment (50 min). PFI-containing blends were prepared 24 h prior to device fabrication by mixing PEDOT:PSS (CLEVIOS P VP AI 4083) with Nafion in a 1:6:14 ratio and diluted in deionized water (1:1). PEDOT:PSS:PFI was applied by spin coating, resulting in films of 20 nm thickness, which were subsequently annealed at 130 °C for 12 min. The substrates were then transferred to a nitrogen-filled glove box. Thermal evaporation of the emissive layer was performed at a base pressure of 2×10^{-6} to 3×10^{-6} mbar. Barium (2.5 nm) and aluminum

(100 nm) were evaporated to finalize the top contact. For hole-only devices, a top contact consisting of C_{60} (4 nm), MoO_3 (10 nm), and aluminum (100 nm) was evaporated. For electron-only devices, aluminum (30 nm) was thermally evaporated on cleaned glass substrates, followed by thermal evaporation of the emissive layer and a TPBi (4 nm) interlayer and the barium (5 nm) and aluminum (100 nm) top contact.

Electrical Measurements: Electrical characterization was carried out under nitrogen atmosphere with a Keithley 2400 source meter and light output was recorded with a Si photodiode with NIST-traceable calibration, with a detector area (1 cm^2) larger than the emitting area of the OLED (0.16 cm^2). The photodiode was placed close to (but not in contact with) the OLED to capture all photons emitted in a forward hemisphere. To avoid any light detection emitted from the substrate edges, the edges were masked by the sample holder and the substrate size (3×3 cm^2) was considerably larger than the photodetector area. The EQE, the luminance and power efficiency were calculated from the measured photocurrent, the device current, and the electroluminescence spectrum. Electroluminescence spectra were obtained with a USB4000-UV-VIS-ES spectrometer.

Photophysical Measurements: Photoluminescence quantum yields were determined with a HORIBA Jobin-Yvon Fluorolog 3–22 Tau-3, using an integrating sphere (F-3018) from Horiba and flushing the samples under continuous nitrogen flow. Time-resolved photoluminescence (TRPL) measurements were performed according to a reported procedure.[34]

Supporting Information

Supporting Information is available from the Wiley Online Library or from the author.

Acknowledgements

Open access funding enabled and organized by Projekt DEAL.

Conflict of Interest

The authors declare no conflict of interest.

Data Availability Statement

The data that support the findings of this study are available from the corresponding author upon reasonable request.

Keywords

Drift-diffusion simulations, organic light-emitting diodes, thermally activated delayed fluorescence, Time-resolved photoluminescence

Received: August 16, 2023
Revised: October 23, 2023
Published online: December 3, 2023

[1] C. W. Tang, S. A. Vanslyke, *Appl. Phys. Lett.* **1987**, *51*, 913.
[2] J.-M. Zhuo, L.-H. Zhao, R.-Q. Png, L.-Y. Wong, P.-J. Chia, J.-C. Tang, S. Sivaramakrishnan, M. Zhou, E. C.-W. Ou, S.-J. Chua, W.-S. Sim, L.-L. Chua, P. K.-H. Ho, *Adv. Mater.* **2009**, *21*, 4747.
[3] A. Seemann, T. Sauermann, C. Lungenschmied, O. Armbruster, S. Bauer, H.-J. Egelhaaf, J. Hauch, *Sol. Energy* **2011**, *85*, 1238.
[4] H. T. Nicolai, M. Kuik, G. A. H. Wetzelaer, B. De Boer, C. Campbell, C. Risko, J. L. Brédas, P. W. M. Blom, *Nat. Mater.* **2012**, *11*, 882.
[5] P. K. Nayak, R. Rosenberg, L. Barnea-Nehoshtan, D. Cahen, *Org. Electron.* **2013**, *14*, 966.
[6] G.-J. A. H. Wetzelaer, M. Scheepers, A. M. Sempere, C. Momblona, J. Ávila, H. J. Bolink, *Adv. Mater.* **2015**, *27*, 1837.
[7] I. Rörich, A.-K. Schönbein, D. K. Mangalore, A. Halda Ribeiro, C. Kasparek, C. Bauer, N. I. Craciun, P. W. M. Blom, C. Ramanan, *J. Mater. Chem. C* **2018**, *6*, 10569.
[8] Y. Li, N. B. Kotadiya, B. Van Der Zee, P. W. M. Blom, G.-J. A. H. Wetzelaer, *Adv. Opt. Mater.* **2021**, *9*, 2001812.
[9] B. Ruhstaller, T. Beierlein, H. Riel, S. Karg, J. C. Scott, W. Riess, *IEEE J. Sel. Top. Quantum Electron.* **2003**, *9*, 723.
[10] B. Perucco, N. A. Reinke, D. Rezzonico, E. Knapp, S. Harkema, B. Ruhstaller, *Org. Electron.* **2012**, *13*, 1827.
[11] N. Chopra, J. Lee, Y. Zheng, S.-H. Eom, J. Xue, F. So, *ACS Appl. Mater. Interfaces* **2009**, *1*, 1169.
[12] V. I. Adamovich, S. R. Cordero, P. I. Djurovich, A. Tamayo, M. E. Thompson, B. W. D'andrade, S. R. Forrest, *Org. Electron.* **2003**, *4*, 77.
[13] C.-H. Shih, P. Rajamalli, C.-A. Wu, W.-T. Hsieh, C.-H. Cheng, *ACS Appl. Mater. Interfaces* **2015**, *7*, 10466.
[14] J. Kido, M. Kimura, K. Nagai, *Science (80-.)* **1995**, *267*, 1332.
[15] N. B. Kotadiya, A. Mondal, P. W. M. Blom, D. Andrienko, G.-J. A. H. Wetzelaer, *Nat. Mater.* **2019**, *18*, 1182.
[16] N. B. Kotadiya, A. Mondal, P. W. M. Blom, D. Andrienko, G.-J. A. H. Wetzelaer, *Nat. Mater.* **2019**, *18*, 1182.
[17] T.-L. Wu, M.-J. Huang, C.-C. Lin, P.-Y. Huang, T.-Y. Chou, R.-W. Chen-Cheng, H.-W. Lin, R.-S. Liu, C.-H. Cheng, *Nat. Photonics* **2018**, *12*, 235.
[18] N. B. Kotadiya, P. W. M. Blom, G.-J. A. H. Wetzelaer, *Nat. Photonics* **2019**, *13*, 765.
[19] H. Uoyama, K. Goushi, K. Shizu, H. Nomura, C. Adachi, *Nature* **2012**, *492*, 234.
[20] N. B. Kotadiya, H. Lu, A. Mondal, Y. Ie, D. Andrienko, P. W. M. Blom, G.-J. A. H. Wetzelaer, *Nat. Mater.* **2018**, *17*, 329.
[21] O. Sachnik, X. Tan, D. Dou, C. Haese, N. Kinaret, K.-H. Lin, D. Andrienko, M. Baumgarten, R. Graf, G.-J. A. H. Wetzelaer, J. J. Michels, P. W. M. Blom, *Nat. Mater.* **2023**, *22*, 1114.
[22] D. R. Lee, M. Kim, S. K. Jeon, S.-H. Hwang, C. W. Lee, J. Y. Lee, *Adv. Mater.* **2015**, *27*, 5861.
[23] M. Godumala, S. Choi, S. Y. Park, M. J. Cho, H. J. Kim, D. H. Ahn, J. S. Moon, J. H. Kwon, D. H. Choi, *Chem. Mater.* **2018**, *30*, 5005.
[24] G. H. Kim, R. Lampande, J. B. Im, J. M. Lee, J. Y. Lee, J. H. Kwon, *Mater. Horiz.* **2017**, *4*, 619.
[25] W. H. Lee, D. H. Kim, P. Justin Jesuraj, H. Hafeez, J. C. Lee, D. K. Choi, T.-S. Bae, S. M. Yu, M. Song, C. S. Kim, S. Y. Ryu, *Mater. Res. Express* **2018**, *5*, 076201.
[26] J. Lee, J.-I. Lee, J. Y. Lee, H. Y. Chu, *Appl. Phys. Lett.* **2009**, *94*, 193305.
[27] X. Zhou, D. S. Qin, M. Pfeiffer, J. Blochwitz-Nimoth, A. Werner, J. Drechsel, B. Maennig, K. Leo, M. Bold, P. Erk, H. Hartmann, *Appl. Phys. Lett.* **2002**, *81*, 4070.
[28] H. S. Kim, S.-R. Park, M. C. Suh, *J. Phys. Chem. C* **2017**, *121*, 13986.
[29] H. Nakanotani, K. Masui, J. Nishide, T. Shibata, C. Adachi, *Sci. Rep.* **2013**, *3*, 2127.
[30] L. Porrès, A. Holland, L.-O. Pålsson, A. P. Monkman, C. Kemp, A. Beeby, *J. Fluoresc.* **2006**, *16*, 267.
[31] O. Sachnik, Y. Li, X. Tan, J. J. Michels, P. W. M. Blom, G.-J. A. H. Wetzelaer, *Adv. Mater.* **2023**, *35*, 2300574.
[32] D. Trieb, P. W. M. Blom, G. J. A. H. Wetzelaer, *Adv. Mater. Interfaces* **2023**, *10*, 2202424.
[33] Y. Li, O. Sachnik, B. van der Zee, K. Thakur, C. Ramanan, G. J. A. H. Wetzelaer, P. W. M. Blom, *Adv. Opt. Mater.* **2021**, *9*, 2101149.
[34] K. Thakur, B. van der Zee, G. J. A. H. Wetzelaer, C. Ramanan, P. W. M. Blom, *Adv. Opt. Mater.* **2022**, *10*, 2101784.

[35] S. Sem, S. Jenatsch, K. Stavrou, A. Danos, A. P. Monkman, B. Ruhstaller, *J. Mater. Chem. C* **2022**, *10*, 4878.
[36] Y. Mei, D. Liu, J. Li, J. Wang, *J. Mater. Chem. C* **2022**, *10*, 16524.
[37] Y. J. Cho, K. S. Yook, J. Y. Lee, *Adv. Mater.* **2014**, *26*, 4050.
[38] W. S. Jeon, T. J. Park, S. Y. Kim, R. Pode, J. Jang, J. H. Kwon, *Org. Electron.* **2009**, *10*, 240.
[39] C.-H. Chang, M.-C. Kuo, W.-C. Lin, Y.-T. Chen, K.-T. Wong, S.-H. Chou, E. Mondal, R. C. Kwong, S. Xia, T. Nakagawa, C. Adachi, *J. Mater. Chem.* **2012**, *22*, 3832.
[40] G. A. H. Wetzelaer, *Phys. Rev. Appl.* **2020**, *13*, 034069.
[41] B. Van Der Zee, Y. Li, G.-J. A. H. Wetzelaer, P. W. M. Blom, *Adv. Electron. Mater.* **2022**, *8*, 2101261.